

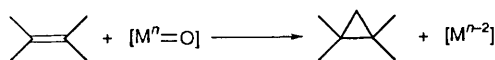
Syntheses of Novel Monomeric 1,4,7-Trimethyl-1,4,7-triazacyclononane Ruthenium Complexes. Reactivities and Structure of Sterically Encumbered Cationic Monoaquaruthenium(II) and Monooxoruthenium(IV) Complexes†

Wing-Chi Cheng, Wing-Yiu Yu, Kung-Kai Cheung and Chi-Ming Che*

Department of Chemistry, The University of Hong Kong, Pokfulam Road, Hong Kong

The complexes $[\text{Ru}^{\text{II}}(\text{tacn})(\text{bipy})(\text{OH}_2)]^{2+}$ **1** and $[\text{Ru}^{\text{IV}}(\text{tacn})(\text{bipy})\text{O}]^{2+}$ **2** (tacn = 1,4,7-trimethyl-1,4,7-triazacyclononane, bipy = 2,2'-bipyridine) have been synthesised and their crystal structures determined: **1**, monoclinic, space group $C2/c$, $a = 34.093(4)$, $b = 10.430(1)$, $c = 17.369(2)$ Å, $\beta = 118.54(1)^\circ$ and $Z = 8$; **2**, triclinic, space group $P\bar{1}$, $a = 10.795(1)$, $b = 11.076(2)$, $c = 11.248(1)$ Å, $\alpha = 110.41(2)$, $\beta = 90.66(1)$, $\gamma = 94.11(1)^\circ$ and $Z = 2$. The structures reveal that tacn acts as a facial chelating ligand with bipy nearly perpendicular to the Ru=O and Ru-OH₂ moieties. The Ru^{IV}=O and Ru-OH₂ distances are 1.815(6) and 2.168(3) Å respectively. In aqueous solution both complexes display two reversible proton-coupled one-electron redox couples corresponding to the oxidation of Ru^{II} to Ru^{III} and Ru^{III} to Ru^{IV}. Complex **2** has been found to be a competent oxidant for alkene epoxidation. Preliminary kinetic studies revealed the rate law, $\text{rate} = k_2[\text{Ru}^{\text{IV}}][\text{alkene}]$ where k_2 at 299 K are $(1.30 \pm 0.11) \times 10^{-3}$ and $(2.52 \pm 0.20) \times 10^{-4} \text{ dm}^3 \text{ mol}^{-1} \text{ s}^{-1}$ for the epoxidation of styrene and norbornene respectively. The activation parameters have been measured and are discussed.

Metal-catalysed formation of epoxides from alkenes¹ has been an important area of research, not only because epoxides are important intermediates for syntheses of many biologically important molecules, but it also poses an intriguing challenge to the mechanism of oxygen atom transfer where two carbon atoms of an alkene are functionalized in a single step (Scheme 1).



Scheme 1

Among the various catalytic systems, metalloporphyrin complexes have received the most extensive investigation.² With sterically bulky and chiral metalloporphyrins as catalysts, shape-selective³ and asymmetric epoxidation⁴ of alkenes have been observed. It is believed that the epoxidation of alkenes by hypervalent oxometalloporphyrin species proceeds through a concerted oxygen-atom abstraction pathway⁵ and the selectivity was explained on the basis of van der Waals interaction between the alkene molecule and the substituents on the porphyrin ring.

The use of oxoruthenium complexes for selective oxidation of hydrocarbons is particularly appealing.⁶ Mechanistic studies by various groups revealed that the oxidation of alkenes by oxoruthenium(IV) complexes are usually accompanied by a large, negative entropy of activation, implying a large orientation demand for the oxidation to occur.^{7,8d,e,9} We anticipate that introduction of sterically bulky group(s) into the co-ordination sphere of the oxoruthenium oxidant could influence the stereochemical course of the reaction similar to that with metalloporphyrin complexes. 1,4,7-Trimethyl-1,4,7-triazacyclononane (tacn) has been reported by Wieghardt and

co-workers¹⁰ to stabilize high-valent Ru^{IV}-O-Ru^{IV} complexes. On the other hand, the steric bulk of the tertiary amine ligand suggests it as a prospective ligand for sterically encumbered oxoruthenium complexes for use in selective oxidation. Herein is described the synthesis and X-ray crystal analyses of monomeric aqua- and oxo-ruthenium complexes of the facially co-ordinating tacn ligand. The complex $[\text{Ru}^{\text{IV}}(\text{tacn})(\text{bipy})\text{O}]^{2+}$ (bipy = 2,2'-bipyridine) has been found to be a selective oxidant for alkene epoxidation.

Experimental

Materials.—The ligand 1,4,7-trimethyl-1,4,7-triazacyclononane (tacn) was prepared as previously reported.¹¹ The compound $\text{RuCl}_3 \cdot 3\text{H}_2\text{O}$ and 2,2'-bipyridine were obtained from Aldrich. Zinc metal (BDH) was used as received. Deionised water was distilled from alkaline potassium permanganate. Acetonitrile used in kinetic experiments was distilled first from alkaline potassium permanganate, then over CaH_2 . All other solvents and chemicals used in syntheses were analytical grade and used without further purification.

Preparations.—The complex $[\text{Ru}(\text{tacn})\text{Cl}_3]$ was synthesised according to the published method.¹²

$[\text{Ru}^{\text{II}}(\text{tacn})(\text{bipy})(\text{OH}_2)][\text{ClO}_4]_2$ **1**. A mixture of $[\text{Ru}(\text{tacn})\text{Cl}_3]$ (50 mg), bipy (20 mg) and zinc metal powder (200 mg) in water (20 cm³) was refluxed for 1 h. The reaction mixture gradually turned red. After cooling, the mixture was filtered to remove the zinc metal and unreacted ligand. A saturated NaClO_4 solution (2 cm³) was added and the solution was left in a refrigerator overnight to afford a dark red microcrystalline solid. This was collected on a frit and washed with a small amount of cold water. Yield: 64 mg (75%) (Found: C, 35.70; H, 4.60; N, 11.25. Calc. for $\text{C}_{19}\text{H}_{31}\text{Cl}_2\text{N}_5\text{O}_9\text{Ru}$: C, 35.35, H, 4.85; N, 10.85%). Ultraviolet-visible [in water, $\lambda_{\text{max}}/\text{nm}(\epsilon_{\text{max}}/\text{dm}^3 \text{ mol}^{-1} \text{ cm}^{-1})$]: 245 (10 250), 300 (25 600), 351 (4780) and 501 (4330).

$[\text{Ru}^{\text{IV}}(\text{tacn})(\text{bipy})\text{O}][\text{ClO}_4]_2$ **2**. The complex $[\text{Ru}^{\text{II}}(\text{tacn})$

† Supplementary data available: see instructions for Authors, *J. Chem. Soc., Dalton Trans.*, 1994, Issue 1, pp. xxiii–xxviii.

(bipy)(OH₂)[ClO₄]₂ (50 mg) was dissolved in deionised water (10 cm³). The solution was cooled in an ice-bath and an aqueous solution of [NH₄]₂[Ce(NO₃)₆] (200 mg in 5 cm³) was added. The solution changed immediately from deep red to light orange. A yellowish brown solid was precipitated upon addition of NaClO₄. Yield: 35 mg (70%) (Found: C, 35.80; H, 4.55; N, 11.40. Calc. for C₁₉H₂₉Cl₂N₅O₉Ru: C, 35.45; H, 4.55; N, 10.90%). Ultraviolet-visible [in water, λ_{max}/nm(ε_{max}/dm³ mol⁻¹ cm⁻¹): 314 (25 200).

Stoichiometric Oxidation.—Stoichiometric oxidation was performed by dissolving complex **2** (30 mg) in degassed acetonitrile (4 cm³) containing an alkene (100 mg). The reaction mixture was stirred at room temperature with a Teflon-coated magnetic stirrer under a nitrogen atmosphere. A control experiment in the absence of the metal oxidant was performed for each reaction. The organic products were analysed by gas chromatography, ¹H NMR and mass spectrometry. Gas chromatographic analyses were conducted by using a Hewlett-Packard 5890 series II chromatograph with a flame ionisation detector, HP-17 column (cross-linked 50% methyl phenyl silicone, film thickness 0.2 μm) and high-purity nitrogen as the carrier gas. Components were identified by comparing retention times with those of authentic samples as well as by gas chromatographic-mass spectral analysis. Quantification of individual gas chromatographic components was by the internal standard method employing a Hewlett-Packard 3396 series II electronic integrator.

Physical Measurements and Instrumentation.—The UV/VIS spectra were recorded on a Milton Roy (Spectronic 3000 array) diode-array spectrophotometer, IR spectra on a Nicolet model 20 FXT FT-IR spectrophotometer as Nujol mulls (4000–400 cm⁻¹) and ¹H NMR spectra on a JEOL model FX 270 Q spectrometer. Cyclic voltammograms were recorded on a Princeton Applied Research model 173 potentiostat and 175 universal programmer using an edge-plane pyrolytic graphite working electrode and a saturated calomel reference electrode (SCE).

Kinetics was studied by the use of a Perkin-Elmer Lambda 3B UV/VIS spectrophotometer. The temperature of the solution was maintained to ±0.1 °C with a water-bath (bath and circulator model 2800, Masterline Fourma Scientific). The rate of alkene oxidation was followed by monitoring the increase in absorbance of the ruthenium(II) complex at 458 nm in acetonitrile under the condition that the alkene was in at least 100-fold excess (*i.e.* pseudo-first-order conditions).

X-Ray Structure Analysis.—X-Ray diffraction data for [Ru(tacn)(bipy)(OH₂)]₂[ClO₄]₂·2H₂O and [Ru(tacn)(bipy)-O][ClO₄]₂ were collected on an Enraf-Nonius CAD4 diffractometer with graphite-monochromated Mo-Kα radiation using the ω-2θ scan method.

Crystal data. 1·2H₂O, C₁₉H₃₁Cl₂N₅O₉Ru·2H₂O, *M_r* = 681.94, monoclinic, space group *C2/c*, *a* = 34.093(4), *b* = 10.430(1), *c* = 17.369(2) Å, β = 118.54(1)°, *U* = 5425.8(1.0) Å³, *Z* = 8, *D_c* = 1.668 g cm⁻³, μ(Mo-Kα) = 8.26 cm⁻¹, *F*(000) = 2800. **2**, C₁₉H₂₉Cl₂N₅O₉Ru, *M_r* = 643.45, triclinic, space group *P1̄*, *a* = 10.795(1), *b* = 11.076(2), *c* = 11.248(1) Å, α = 110.41(2), β = 90.66(1), γ = 94.11(1)°, *U* = 1256.1(1.0) Å³, *Z* = 2, *D_c* = 1.701 g cm⁻³, μ(Mo-Kα) = 8.82 cm⁻¹, *F*(000) = 656. Crystals of dimensions 0.1 × 0.15 × 0.15 mm for 1·2H₂O and 0.15 × 0.15 × 0.2 mm for **2** were used for data collection at 23 °C.

Intensity data (1·2H₂O, 2θ_{max} = 44°, *h* 0–36, *k* 0–11, *l* –18 to 18; **2**, 2θ_{max} = 48°, *h* 0–12, *k* –12 to 12, *l* –12 to 12) were corrected for Lorentz and polarisation effects and empirical absorption based on the Ψ scan of eight strong reflections. For 1·2H₂O, 3544 independent reflections were obtained, 2559 with *F_o* > 6.0σ(*F_o*) being considered observed and used in the structural analysis. For **2** the numbers of independent and

observed [*F_o* > 6.0σ(*F_o*)] reflections were 3936 and 2342. The space groups of both complexes were determined from systematic absences and the structures were solved by Patterson and Fourier methods and subsequent refinement by full-matrix least squares using the Enraf-Nonius programs¹³ on a MicroVAX II computer. Each of the two perchlorate ions was disordered with respect to one oxygen atom and the disordered O atoms were only refined isotropically. The hydrogen atoms of the aqua oxygen O(1) and one of the water molecules were located in the Fourier difference synthesis and the positional parameters refined. The H atoms of the second water molecule were not located. All the other H atoms at calculated positions with isotropic thermal parameters equal to 1.3 times that of the attached C atom were not refined. All other atoms were refined anisotropically. For 1·2H₂O, convergence for 353 variables by least-squares refinement of *F* with *w* = 4*F_o*²/σ²(*F_o*²), where σ²(*F_o*²) = [σ²(*I*) + (0.040 *F_o*²)²] was reached at *R* = 0.037, *R'* = 0.048 and *S* = 1.691 for the 2559 reflections; (Δ/σ)_{max} = 0.02 atoms of the complex cation. The final Fourier difference map was featureless, with maximum positive and negative peaks of 0.97 and 0.67 e Å⁻³ respectively. The distance between the O atoms of the water molecules is 2.74(1) Å and there are several intermolecular distances of about 3.3 Å involving the O atoms of the perchlorate ions and non-hydrogen atoms of the complex cation. For **2** the final refinement was reached at *R* = 0.051, *R'* = 0.057 and *S* = 1.401 for the 2342 observed reflections and 323 variables; (Δ/σ)_{max} = 0.03 for atoms of the complex cation. A final Fourier difference map was featureless, with maximum positive and negative peaks of 1.00 and 0.62 e Å⁻³ respectively. There are several intermolecular distances from 3.2 to 3.4 Å involving the O atoms of the perchlorate ions and non-H atoms of the complex cation.

Atomic coordinates of non-hydrogen atoms are listed in Table 1, selected bond distances and angles in Tables 2 and 3.

Additional material available from the Cambridge Crystallographic Data Centre comprises H-atom coordinates, thermal parameters and remaining bond lengths and angles.

Results and Discussion

Syntheses and Characterization.—The synthesis of Ru=O complexes having a facially chelating tridentate ligand is not unprecedented. Meyer and co-workers¹⁴ had isolated [Ru^{IV}(tpzm)(bipy)O]²⁺ [tpzm = tris(1-pyrazolyl)methane] in which tpzm acts as a facially chelating ligand. In this work, [Ru(tacn)Cl₃] was chosen as the starting material. Its reduction by zinc metal powder in the presence of a stoichiometric amount of 2,2'-bipyridine in hot water gave [Ru^{II}(tacn)(bipy)(OH₂)]²⁺ **1** in good yield. Water is an important solvent for the success of the synthesis. Attempts to use absolute ethanol as solvent together with either triethylamine or zinc metal as the reductant did not afford the desired product. Triethylamine, which is used as a reductant in the preparation of [Ru^{II}(terpy)(α-diimine)Cl]⁺ (terpy = 2,2':6',2''-terpyridine) from [Ru(terpy)Cl₃]³⁺,¹⁵ was found to be ineffective for the reduction of [Ru(tacn)Cl₃]. Presumably, tacn is a stronger σ donor which would lower the *E*^o(Ru^{III}–Ru^{II}) value. Seemingly, zinc metal is an appropriate choice. This method directly gave the aquaruthenium complex and subsequent oxidation by Ce^{IV} led to [Ru^{IV}(tacn)(bipy)O]²⁺ **2** isolated as a yellowish brown ClO₄⁻ salt.

The UV/VIS spectrum of complex **1** in water [Fig. 1(a)] displays intense absorption bands at 245, 300, 351 and 501 nm with the last being characteristic Ru^{II} → π*(bipy) metal-to-ligand charge-transfer (m.l.c.t.) transition. That the m.l.c.t. transition is red-shifted from that of the terpy analogue (λ_{max} = 477 nm) can be rationalised by the stronger σ-donor strength of tacn, which would destabilise the d_π(Ru) orbitals. Fig. 1(b) depicts the UV/VIS spectrum of complex **2**, which is featureless with the complete absence of the m.l.c.t. bands. The IR spectrum shows an intense absorption at 780 cm⁻¹ which is

conspicuously absent for **1**. This is tentatively assigned to the $\text{Ru}^{\text{IV}}=\text{O}$ stretch based on previous work on other monooxoruthenium(IV) complexes. The measured μ_{eff} of $2.83 \mu_{\text{B}}$ is a characteristic feature of the $(d_{xy})^2(d_{xz})^1(d_{yz})^1$ electronic configuration of the oxoruthenium(IV) system.⁶

Crystal Structures.—Perspective drawings of the cations $[\text{Ru}(\text{tacn})(\text{bipy})(\text{OH}_2)]^{2+}$ **1** and $[\text{Ru}(\text{tacn})(\text{bipy})\text{O}]^{2+}$ **2** are shown in Figs. 2 and 3 respectively. Both complexes display similar structure. The co-ordination geometry about the Ru atom in each case is distorted octahedral. As expected, the tacn facially co-ordinates to Ru with N(2) *trans* to the oxygen atom of the co-ordinated water molecule and the oxo-group. In **1** the Ru–OH₂ distance of 2.168(3) Å is comparable to that of 2.122(16) Å in $[\text{Ru}(\text{OH}_2)_6]^{2+}$,¹⁶ and 2.151(7) Å in $[\text{Ru}(\text{terpy})(\text{tmen})(\text{OH}_2)]^{2+}$ (tmen = *N,N,N',N'*-tetramethylethylenediamine).¹⁷ For **2** the bipyridine is essentially perpendicular to the oxo-moiety [N(4)–Ru–O(1) 92.2(3), N(5)–Ru–O(1) 90.4(3)°]. The Ru=O distance of 1.815(6) Å is 0.05 Å longer than that in $[\text{RuL}'(\text{O})(\text{MeCN})]^{2+}$, (L' =

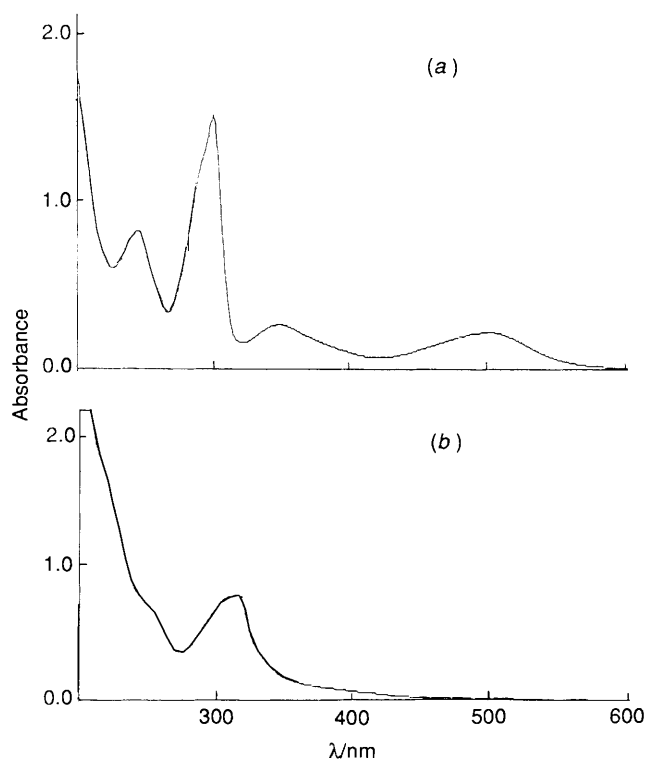


Fig. 1 The UV/VIS spectra of (a) $[\text{Ru}(\text{tacn})(\text{bipy})(\text{OH}_2)]^{2+}$ and (b) $[\text{Ru}(\text{tacn})(\text{bipy})\text{O}]^{2+}$ in water

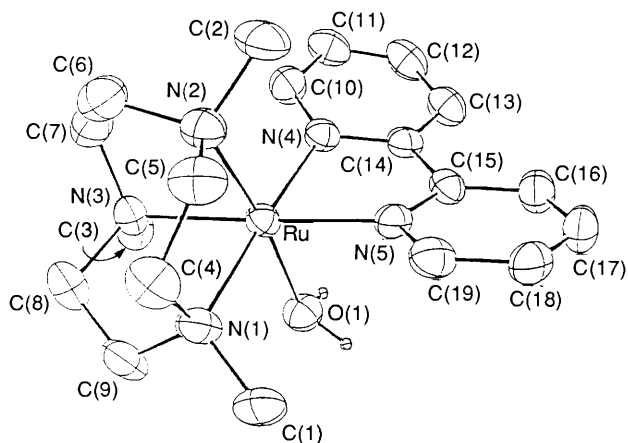


Fig. 2 A perspective drawing of the $[\text{Ru}(\text{tacn})(\text{bipy})(\text{OH}_2)]^{2+}$ cation

1,4,8,11-tetramethyl-1,4,8,11-tetraazacyclotetradecane).¹⁸ As a comparison, the Ru^{IV}–O (bridging) distances of the dimeric complex $[(\text{tacn})\text{Ru}(\mu\text{-O})_3\text{Ru}(\text{tacn})]^{2+}$ reported by Wiegardt and co-workers,¹⁰ range from 1.899(9) to 1.937(9) Å. The Ru–N(1) and Ru–N(3) distances are not affected after oxidation of **1** to **2**. However, Ru–N(2), which is *trans* to the oxo group, is substantially lengthened by 0.096 Å. This is in accord with the significant *trans* influence of the oxo ligand.

Electrochemistry in Aqueous Media.—The electrochemistry of a number of oxoruthenium(IV) complexes has been reported and discussed.^{8d,e,9} In this work the cyclic voltammograms of **1** and **2** in aqueous solutions are virtually identical. A typical voltammogram of **1** at pH 1.1 (0.1 mol dm⁻³ CF₃CO₂H) is

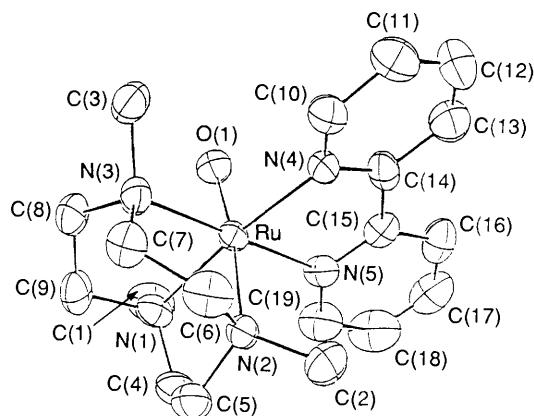


Fig. 3 A perspective drawing of the $[\text{Ru}(\text{tacn})(\text{bipy})\text{O}]^{2+}$ cation

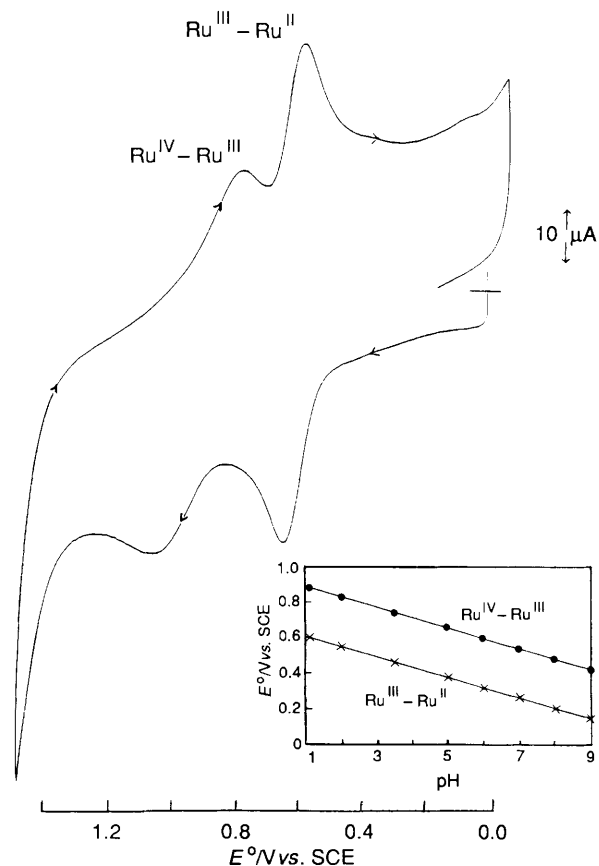


Fig. 4 Cyclic voltammogram of $[\text{Ru}(\text{tacn})(\text{bipy})(\text{OH}_2)]^{2+}$ in 0.1 mol dm⁻³ CF₃CO₂H at pH 1.1 (*vs.* SCE) with an edge-plane pyrolytic graphite working electrode at scan rate 50 mV s⁻¹. Insert shows plots of *E*⁰ *vs.* pH for the Ru^{III}–Ru^{II} and Ru^{IV}–Ru^{III} couples of $[\text{Ru}(\text{tacn})(\text{bipy})(\text{OH}_2)]^{2+}$

Table 1 Atomic coordinates of non-hydrogen atoms

Atom	x	y	z	Atom	x	y	z
<i>(a) [Ru(tacn)(bipy)(OH₂)] [ClO₄]₂</i>							
Ru	0.134 67(1)	0.198 21(4)	0.334 62(2)	N(5)	0.087 4(1)	0.252 4(5)	0.372 1(2)
Cl(1)	0.211 95(5)	0.355 5(2)	0.821 37(9)	C(1)	0.172 1(2)	0.051 9(7)	0.512 6(3)
Cl(2)	0.451 93(4)	0.289 4(1)	0.052 16(9)	C(2)	0.051 1(2)	0.094 4(7)	0.185 6(4)
O(1)	0.179 6(1)	0.334 8(4)	0.430 0(2)	C(3)	0.210 7(2)	0.256 1(6)	0.292 9(4)
O(11)	0.187 0(2)	0.421 4(5)	0.855 2(3)	C(4)	0.142 5(2)	-0.079 9(6)	0.379 5(4)
O(12)	0.183 3(2)	0.277 0(4)	0.749 8(3)	C(5)	0.096 5(2)	-0.053 4(6)	0.304 2(4)
O(13)	0.233 2(1)	0.446 9(5)	0.792 8(3)	C(6)	0.120 0(2)	0.004 9(6)	0.196 1(3)
O(14)	0.248 3(3)	0.282 4(9)	0.881 7(6)	C(7)	0.155 0(2)	0.097 5(6)	0.200 4(3)
O(15)	0.240 5(3)	0.270 6(9)	0.894 0(6)	C(8)	0.212 6(2)	0.042 3(6)	0.384 4(4)
O(21)	0.464 8(2)	0.203 1(6)	0.009 3(3)	C(9)	0.213 3(2)	0.040 1(6)	0.434 8(3)
O(22)	0.476 3(7)	0.285 3(7)	0.141 4(3)	C(10)	0.108 7(2)	0.403 9(6)	0.186 5(3)
O(23)	0.426 9(3)	0.383 5(9)	0.014 0(5)	C(11)	0.092 5(2)	0.518 8(6)	0.147 0(4)
O(24)	0.413 5(4)	0.224(1)	0.050 5(7)	C(12)	0.071 5(2)	0.597 1(6)	0.180 6(4)
O(25)	0.471 8(5)	0.397(2)	0.031 1(9)	C(13)	0.066 2(2)	0.554 5(6)	0.249 5(1)
O(30)	0.167 7(1)	0.385 1(5)	0.569 8(3)	C(14)	0.081 6(2)	0.432 9(5)	0.284 3(3)
O(31)	0.170 3(2)	0.647 6(6)	0.568 2(4)	C(15)	0.071 6(2)	0.373 4(5)	0.348 0(3)
N(1)	0.167 0(1)	0.041 4(5)	0.423 4(3)	C(16)	0.043 8(2)	0.429 1(6)	0.377 1(3)
N(2)	0.097 8(1)	0.052 2(5)	0.248 0(3)	C(17)	0.030 7(2)	0.361 6(6)	0.428 6(4)
N(3)	0.182 5(1)	0.147 7(4)	0.292 3(3)	C(18)	0.044 7(2)	0.237 7(6)	0.449 6(3)
N(4)	0.104 8(1)	0.358 3(4)	0.255 4(3)	C(19)	0.073 1(2)	0.185 9(6)	0.420 4(3)
<i>(b) [Ru(tacn)(bipy)O] [ClO₄]₂</i>							
Ru	0.221 77(7)	0.211 59(7)	0.151 23(7)	C(1)	0.413 9(9)	0.102 5(9)	0.281(1)
Cl(1)	0.258 5(2)	0.522 3(2)	0.762 4(2)	C(2)	0.277(1)	0.501 7(8)	0.190 5(9)
Cl(2)	0.268 3(3)	0.850 0(2)	0.486 9(2)	C(3)	-0.045 1(8)	0.127 4(9)	0.209 0(8)
O(1)	0.205 5(6)	0.036 7(6)	0.079 1(5)	C(4)	0.403 2(9)	0.337 9(8)	0.363 0(9)
O(11)	0.228 (1)	0.521(1)	0.880 4(8)	C(5)	0.318 0(9)	0.448 5(8)	0.379 1(8)
O(12)	0.165 4(7)	0.446 2(7)	0.670 2(6)	C(6)	0.103 7(8)	0.443 0(8)	0.301 3(9)
O(13)	0.372 4(8)	0.471 6(9)	0.730(1)	C(7)	0.045 9(8)	0.343 2(8)	0.352 2(8)
O(14)	0.284(1)	0.644(1)	0.738(1)	C(8)	0.121 4(9)	0.138 6(8)	0.355 8(8)
O(15)	0.253(1)	0.658(1)	0.794(1)	C(9)	0.241 3(9)	0.195 1(9)	0.413 1(8)
O(21)	0.250 1(8)	0.870 5(9)	0.368 9(8)	C(10)	0.004 3(9)	0.256 6(9)	-0.011 1(8)
O(22)	0.172(1)	0.758 8(8)	0.494 2(8)	C(11)	-0.051(1)	0.253(1)	-0.122 3(9)
O(23)	0.382 9(9)	0.785(1)	0.463(1)	C(12)	0.014(1)	0.228(1)	-0.227(1)
O(24)	0.268(2)	0.970(2)	0.570(2)	C(13)	0.137(1)	0.208 5(9)	-0.221 9(9)
O(25)	0.296(1)	0.937(2)	0.607(1)	C(14)	0.189 8(9)	0.214 9(8)	-0.107 0(7)
N(1)	0.329 6(7)	0.211 7(6)	0.312 2(6)	C(15)	0.324 6(8)	0.212 5(8)	-0.090 6(8)
N(2)	0.234 6(7)	0.418 1(6)	0.261 5(6)	C(16)	0.406(1)	0.204 9(9)	-0.187 8(9)
N(3)	0.072 4(7)	0.207 6(7)	0.274 3(6)	C(17)	0.532(1)	0.210(1)	-0.162(1)
N(4)	0.122 9(6)	0.233 9(6)	-0.003 0(6)	C(18)	0.572(1)	0.221(1)	-0.044(1)
N(5)	0.365 6(6)	0.221 1(7)	0.027 2(6)	C(19)	0.488 3(9)	0.227(1)	0.050(1)

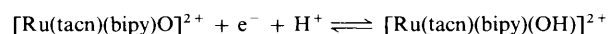
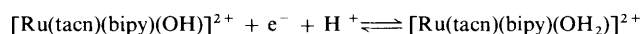
Table 2 Selected bond distances (Å) and angles (°) in [Ru(tacn)-(bipy)(OH₂)]²⁺

Ru-O(1)	2.168(3)	Ru-N(3)	2.149(5)
Ru-N(1)	2.154(4)	Ru-N(4)	2.093(5)
Ru-N(2)	2.087(4)	Ru-N(5)	2.083(5)
O(1)-Ru-N(1)	91.1(1)	N(1)-Ru-N(5)	100.9(2)
O(1)-Ru-N(2)	173.3(2)	N(2)-Ru-N(3)	82.4(2)
O(1)-Ru-N(3)	92.8(2)	N(2)-Ru-N(4)	99.9(2)
O(1)-Ru-N(4)	85.5(1)	N(2)-Ru-N(5)	97.7(2)
O(1)-Ru-N(5)	87.3(2)	N(3)-Ru-N(4)	100.4(2)
N(1)-Ru-N(2)	83.6(2)	N(3)-Ru-N(5)	178.0(2)
N(1)-Ru-N(3)	81.1(2)	N(4)-Ru-N(5)	77.6(2)
N(1)-Ru-N(4)	176.3(2)		

Table 3 Selected bond distances (Å) and angles (°) in [Ru(tacn)(bipy)O]²⁺

Ru-O(1)	1.815(6)	Ru-N(3)	2.145(8)
Ru-N(1)	2.141(7)	Ru-N(4)	2.123(7)
Ru-N(2)	2.183(6)	Ru-N(5)	2.121(8)
O(1)-Ru-N(1)	94.1(3)	N(1)-Ru-N(5)	100.2(3)
O(1)-Ru-N(2)	172.4(3)	N(2)-Ru-N(3)	82.7(3)
O(1)-Ru-N(3)	91.0(3)	N(2)-Ru-N(4)	93.3(3)
O(1)-Ru-N(4)	92.2(3)	N(2)-Ru-N(5)	96.0(3)
O(1)-Ru-N(5)	90.4(3)	N(3)-Ru-N(4)	100.5(3)
N(1)-Ru-N(2)	80.7(3)	N(3)-Ru-N(5)	177.6(4)
N(1)-Ru-N(3)	81.5(3)	N(4)-Ru-N(5)	77.7(3)
N(1)-Ru-N(4)	173.4(3)		

shown in Fig. 4. It reveals two couples: a reversible wave at 0.59 V vs. SCE corresponding to the Ru^{III}-Ru^{II} couple and a quasi reversible wave, with a smaller measured current, at 0.90 V is assigned as the Ru^{IV}-Ru^{III} couple. Similar patterns have been observed for [Ru(terpy)(bipy)(OH₂)]²⁺¹⁹ and [Ru(tpzm)-(bipy)(OH₂)]²⁺.¹⁴ Both couples shift cathodically as the pH increases in the range 1 < pH < 9. The Pourbaix diagram for complex 1 is shown as an insert in Fig. 4. The E° values for both couples shift by -60 mV per pH unit over the above-mentioned

**Scheme 2**

pH range. This is consistent with one-electron, one-proton transfer according to Scheme 2.

A comparison of electrochemical data for various 2,2'-

bipyridine analogues of $[\text{RuL}(\text{bipy})(\text{OH}_2)]^{2+}$, where L = tacn, terpy,²⁴ or tpzm,¹⁴ revealed that replacing the pyridyl ligands by tacn leads to a substantial decrease in the E° values of the $\text{Ru}^{\text{IV}}-\text{Ru}^{\text{III}}$ couples. At pH 7.0 $[\text{Ru}(\text{terpy})(\text{bipy})\text{O}]^{2+}$ and $[\text{Ru}(\text{tpzm})(\text{bipy})\text{O}]^{2+}$ are more oxidising than $[\text{Ru}(\text{tacn})(\text{bipy})\text{O}]^{2+}$ [$E^\circ(\text{Ru}^{\text{IV}}-\text{Ru}^{\text{III}}) = 0.54$ V at pH 7] by 80 and 170 mV respectively. This is not unexpected given the fact that *trans*- $[\text{RuL}'\text{O}_2]^{2+}$ (ref. 21) is 340 mV less oxidising than is *trans*- $[\text{Ru}(\text{bipy})_2\text{O}_2]^{2+}$ (ref. 20) at pH 1.

Stoichiometric Oxidation and Reactivities.—Previous findings showed that oxoruthenium(IV) complexes are active stoichiometric oxidants.⁶ Similarly, $[\text{Ru}(\text{tacn})(\text{bipy})\text{O}]^{2+}$ is a competent oxidant of olefins. The results are summarized in Table 4. In each reaction the ruthenium product $[\text{Ru}(\text{tacn})(\text{bipy})(\text{MeCN})]^{2+}$, identified by its m.l.c.t. band at 458 nm, was isolated quantitatively. Complex 2 efficiently oxidised norbornene and styrene to *exo*-epoxynorbornane and styrene oxide (10% benzaldehyde as side product) in 79 and 62% yield respectively. Stereoretentive epoxidation was observed for *cis*- and *trans*-stilbenes. Similar results were also observed by employing $[\text{Ru}(\text{bipy})_2(\text{py})\text{O}]^{2+}$ (py = pyridine)^{7b} and $[\text{Ru}(\text{terpy})(\text{tmchxn})\text{O}]^{2+}$ ²² (tmchxn = *N,N,N',N'*-tetramethyl-1,2-diaminocyclohexane) as the oxidants. In the oxidation of cyclohexene the dominant products were cyclohexen-2-one and cyclohexen-2-ol arising from allylic oxidation. Nevertheless, a noticeable amount of cyclohexene oxide (8%) was found. This is in contrast with the previous findings that oxidation of cyclohexene by oxoruthenium(IV) complexes such as $[\text{Ru}(\text{terpy})(\text{dcbipy})\text{O}]^{2+}$ (dcbipy = 6,6'-dichloro-2,2'-bipyridine)^{8e} would give cyclohexen-2-one exclusively.

Fig. 5 shows the typical UV/VIS spectral changes in the reaction of complex 2 with norbornene in acetonitrile. It represents the clean conversion of $[\text{Ru}(\text{tacn})(\text{bipy})\text{O}]^{2+}$ into $[\text{Ru}(\text{tacn})(\text{bipy})(\text{MeCN})]^{2+}$ with well defined isosbestic points at 305 and 340 nm. Thus the epoxidation was accompanied by the concomitant reduction of Ru^{IV} to Ru^{II} . Kinetic experiments performed in acetonitrile revealed a second-order rate law, rate = $k_2[\text{Ru}(\text{tacn})(\text{bipy})\text{O}]^{2+}[\text{alkene}]$ under the condition that $[\text{alkene}] \gg [\text{Ru}^{\text{IV}}=\text{O}]$. The measured second-order rate

constants (k_2) at 299 K for the epoxidation of styrene and norbornene are $(1.30 \pm 0.11) \times 10^{-3}$ and $(2.52 \pm 0.20) \times 10^{-4}$ $\text{dm}^3 \text{mol}^{-1} \text{s}^{-1}$ respectively. These values are more than 10 times slower than for similar reactions at 298 K with $[\text{Ru}^{\text{IV}}(\text{terpy})(\text{L})\text{O}]^{2+}$ (L = dcbipy, 2.8×10^{-2} $\text{dm}^3 \text{mol}^{-1} \text{s}^{-1}$ in MeCN,^{8e} *N,N,N',N'*-tetramethylethylenediamine, 2.0×10^{-2} $\text{dm}^3 \text{mol}^{-1} \text{s}^{-1}$ in 0.1 mol dm^{-3} HClO_4 ^{8d}) and $[\text{Ru}(\text{bipy})_2(\text{py})\text{O}]^{2+}$ ($k_2 = 1.48 \times 10^{-2}$ $\text{dm}^3 \text{mol}^{-1} \text{s}^{-1}$ in MeCN)^{7b} and are even four times slower than that with $[\text{Ru}(\text{tpp})\text{O}_2]$ [$k_2 = 4.3 \times 10^{-3}$ $\text{dm}^3 \text{mol}^{-1} \text{s}^{-1}$ in CH_2Cl_2 -MeOH (19:1)],²³ where tpp = 5,10,15,20-tetraphenylporphyrinate.

The effect of temperature on the second-order rate constants for norbornene and styrene oxidation by $[\text{Ru}(\text{tacn})(\text{bipy})\text{O}]^{2+}$ has been studied. The ΔH^\ddagger and ΔS^\ddagger values (Table 5) were obtained from the Eyring plots of $\ln(k_2/T)$ vs. $1/T$, which are linear over the temperature range 19–42 °C. The large and negative ΔS^\ddagger values implicitly reveal a large orientation demand for the oxygen-atom transfer.

General Remarks.—The design of a milder oxidant has important implications in selective alkene epoxidation, because it is expected to transfer oxygen to an alkene *via* product-like transition states, resulting in more specific non-bonded interactions; conversely a more reactive oxidant should proceed *via* a more reactant-like transition state, with greater separation between substrate and oxidant and concomitantly poorer steric differentiation. In their studies on asymmetric alkene epoxidation by chiral manganese(III) Schiff-base complexes, Jacobsen *et al.*²⁴ found a better enantiodifferentiation can be obtained from a late (product-like) transition state. In this work, a mild monooxoruthenium(VI) oxidant based on 1,4,7-trimethyl-1,4,7-triazacyclononane and 2,2'-bipyridine has been prepared. For a concerted oxygen-atom transfer the sterically bulky tacn ligand is expected to inhibit free approach of the alkene. Since the Ru=O group is perpendicular to the bipyridine ligand, it is

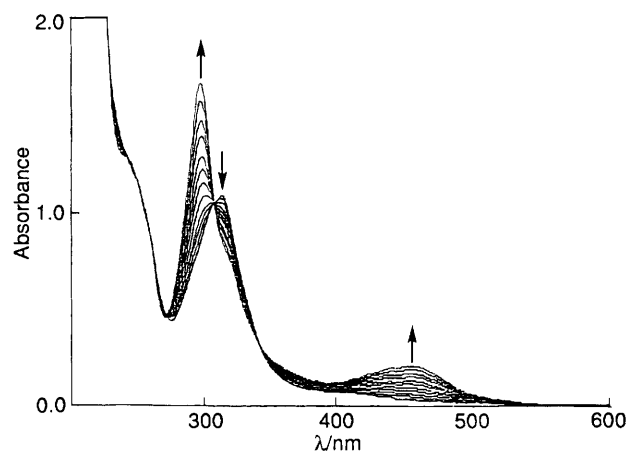


Fig. 5 The UV/VIS spectral changes for the oxidation of norbornene (0.1 mol dm^{-3}) by $[\text{Ru}(\text{tacn})(\text{bipy})\text{O}]^{2+}$ in acetonitrile at room temperature. Scan interval 10 min

Table 4 Oxidation of alkenes (100 mg) by $[\text{Ru}(\text{tacn})(\text{bipy})\text{O}]^{2+}$ (30 mg) in acetonitrile (4 cm^3) under a nitrogen atmosphere for 8 h

Substrate	Products	Yield (%) [*]
Styrene	Styrene oxide	62
	Benzaldehyde	12
<i>trans</i> -Stilbene	<i>trans</i> -Stilbene oxide	18
	Benzaldehyde	< 1
<i>cis</i> -Stilbene	<i>cis</i> -Stilbene oxide	45
	<i>trans</i> -Stilbene oxide	4
Norbornene	<i>exo</i> -2,3-Epoxynorbornane	79
Cyclohexene	Cyclohexene oxide	8
	Cyclohexen-2-ol	30
	Cyclohexen-2-one	62

* Defined as the percentage of moles of product to the moles of ruthenium oxidant used.

Table 5 Second-order rate constants for norbornene and styrene epoxidation by $[\text{Ru}(\text{tacn})(\text{bipy})\text{O}]^{2+}$ in acetonitrile at various temperatures (cal = 4.184 J)

Substrate	T/K	$k_2/\text{dm}^3 \text{mol}^{-1} \text{s}^{-1}$	$\Delta H^\ddagger/\text{kcal mol}^{-1}$	$\Delta S^\ddagger/\text{cal K}^{-1} \text{mol}^{-1}$
Styrene	289.2	$(0.79 \pm 0.03) \times 10^{-3}$	10.1 ± 1.1	−37.9 ± 4.5
	299.2	$(1.30 \pm 0.11) \times 10^{-3}$		
	305.5	$(1.99 \pm 0.07) \times 10^{-3}$		
	314.2	$(3.47 \pm 0.32) \times 10^{-3}$		
Norbornene	299.2	$(2.52 \pm 0.20) \times 10^{-4}$	17.7 ± 2.5	−15.8 ± 3.0
	305.5	$(5.40 \pm 0.58) \times 10^{-4}$		
	310.1	$(8.06 \pm 0.40) \times 10^{-4}$		
	314.2	$(10.79 \pm 0.31) \times 10^{-4}$		

anticipated that the addition of suitable substituents (sterically bulky or chiral appendages) on the bipyridine ligand may lead to regio-, shape- or even enantio-selective alkene epoxidation.

Acknowledgements

We acknowledge support from The University of Hong Kong and the Hong Kong Research Grants Council. W.-C. Cheng acknowledges the receipt of a studentship administered by the Croucher Foundation and Hung Hing Ying Scholarships. W.-Y. Yu is the recipient of a fellowship administered by the Sir Edward Youde Foundation.

References

- 1 K. A. Jørgensen, *Chem. Rev.*, 1989, **3**, 431.
- 2 B. Menuier, *Chem. Rev.*, 1992, **92**, 1441.
- 3 J. T. Groves and T. E. Nemo, *J. Am. Chem. Soc.*, 1983, **105**, 5789; K. S. Suslick and B. R. Cook, *J. Chem. Soc., Chem. Commun.*, 1989, 200; G.-X. He, H.-Y. Mei and T. C. Bruice, *J. Am. Chem. Soc.*, 1991, **113**, 5644.
- 4 J. P. Collman, X. Zhang, V. J. Lee and J. T. Brauman, *J. Chem. Soc., Chem. Commun.*, 1992, 1647 and refs. therein; J. T. Groves and R. S. Myers, *J. Am. Chem. Soc.*, 1983, **105**, 5791; S. O'Malley and T. K. Kodadek, *J. Am. Chem. Soc.*, 1989, **111**, 9116.
- 5 D. Ostovic and T. C. Bruice, *Acc. Chem. Res.*, 1992, **25**, 314.
- 6 W. P. Griffith, *Chem. Soc. Rev.*, 1992, **21**, 179; C. M. Che and V. W. W. Yam, *Adv. Inorg. Chem.*, 1992, **39**, 233.
- 7 See, for example (a) M. S. Thompson, W. F. De Giovanni, B. A. Moyer and T. J. Meyer, *J. Org. Chem.*, 1984, **49**, 4972; (b) J. C. Dobson, W. K. Soek and T. J. Meyer, *Inorg. Chem.*, 1986, **25**, 1514; (c) L. Roecker and T. J. Meyer, *J. Am. Chem. Soc.*, 1987, **109**, 746; (d) R. A. Binstead, M. E. McGuire, A. Dovletoglou, W. K. Seok, L. E. Roecker and T. J. Meyer, *J. Am. Chem. Soc.*, 1992, **114**, 173 and refs. therein.
- 8 (a) C. M. Che and W. O. Lee, *J. Chem. Soc., Chem. Commun.*, 1988, 881; (b) T. C. Lau, C. M. Che, W. O. Lee and C. K. Poon, *J. Chem. Soc., Chem. Commun.*, 1988, 1406; (c) C. M. Che, V. W. W. Yam and T. C. W. Mak, *J. Am. Chem. Soc.*, 1990, **112**, 2284; (d) C. Ho, C. M. Che and T. C. Lau, *J. Chem. Soc., Dalton Trans.*, 1990, 967; (e) C. M. Che, C. Ho and T. C. Lau, *J. Chem. Soc., Dalton Trans.*, 1991, 1901; (f) C. M. Che, W. H. Leung, C. K. Li and C. K. Poon, *J. Chem. Soc., Dalton Trans.*, 1991, 379.
- 9 M. E. Marimion, R. A. Leising and K. J. Takeuchi, *J. Coord. Chem.*, 1988, **19**, 1.
- 10 P. Neubold, B. D. Vedora, K. Wieghardt, B. Nuber and J. Weiss, *Angew. Chem., Int. Ed. Engl.*, 1989, **28**, 763.
- 11 K. Wieghardt, P. Chaudhuri, B. Nuber and J. Wiess, *Inorg. Chem.*, 1982, **21**, 3086.
- 12 P. Neubold, K. Wieghardt, B. Nuber and J. Weiss, *Inorg. Chem.*, 1989, **28**, 459.
- 13 SDP Structure Determination Package, Enraf-Nonius, Delft, 1985.
- 14 A. Lobet, P. Doppelt and T. J. Meyer, *Inorg. Chem.*, 1988, **27**, 514.
- 15 K. J. Takeuchi, M. S. Thompson, D. W. Pipes and T. J. Meyer, *Inorg. Chem.*, 1984, **23**, 1845.
- 16 P. Bernhard, H.-B. Bürgi, J. Hauser, H. Lehmann and A. Ludi, *Inorg. Chem.*, 1982, **21**, 3936.
- 17 N. Grover, N. Gupta, P. Singh and H. H. Thorp, *Inorg. Chem.*, 1992, **31**, 2014.
- 18 C. M. Che, K. Y. Wong and T. C. W. Mak, *J. Chem. Soc., Chem. Commun.*, 1985, 546.
- 19 R. A. Binstead and T. J. Meyer, *J. Am. Chem. Soc.*, 1987, **109**, 3287.
- 20 C. M. Che, K. Y. Wong, W. H. Leung and C. K. Poon, *Inorg. Chem.*, 1986, **25**, 345.
- 21 C. M. Che, T. F. Lai and K. Y. Wong, *Inorg. Chem.*, 1987, **26**, 2289.
- 22 W. Y. Yu and C. M. Che, unpublished work.
- 23 C. Ho, W. H. Leung and C. M. Che, *J. Chem. Soc., Dalton Trans.*, 1991, 2933.
- 24 E. N. Jacobsen, W. Zhang and M. L. Güler, *J. Am. Chem. Soc.*, 1991, **113**, 6703.

Received 29th July 1993; Paper 3/04542K